



## Solar Energy Driven Chemical Looping Air Separation

Y. Görkem Bak , Deniz Üner\* 

<sup>1</sup>Middle East Technical University, Chemical Engineering Department, Ankara, 06800, Türkiye

**Abstract:** Chemical looping is emerging as a feasible alternative to carry out reduction and oxidation processes under different process conditions. This technology proves especially useful when reduction and oxidation processes proceed with different time constants. With the possibility of incorporation of solar energy to the endothermic end of the process, chemical looping technology has recently become more popular. Chemical looping air separation (CLAS) is an alternative to cryogenic separation, by utilizing solar thermal energy. In this process a reducible metal oxide is heated to a temperature such that the metal releases its lattice oxygen. In the second step, the metal oxide is exposed to air and oxygen is captured by the oxide while pure nitrogen is released at the outlet and the loop is closed.  $Mn_2O_3$  is selected as the oxygen carrier to perform chemical looping cycles. Oxygen mobility of the metal oxide and reversibility through redox cycles are tested with thermogravimetric analysis (TGA). The redox cycles are designed such that the air oxidizes, and the steam reduces the material. The reduction behavior of manganese (III) oxide under inert atmosphere is tested in TGA. It is proved that steam acts as an inert gas under the reaction conditions. The use of steam at the reduction stage results in a more convenient separation of the sweep gas (steam) from the oxygen released from the oxide. It is demonstrated that a redox cycle between  $Mn_2O_3$  and  $Mn_3O_4$  can be performed isothermally. The capability of the system to be coupled with solar energy makes it more alluring for environmentally friendly option seekers. The use of solar irradiation is tested with parabolic mirrors to observe the power output. Overall, CLAS process works on milder conditions which is crucial in reducing the energy and equipment costs, and its advantages regarding energy efficiency increase even more when solar energy is incorporated into the system.

**Keywords:** Chemical Looping Air Separation, Solar Energy, Sustainable Production

**Submitted:** December 13, 2013 . **Accepted:** February 06, 2024.

**Cite this:** Bak, Y. G., & Üner, D. (2024). Solar Energy Driven Chemical Looping Air Separation. Journal of the Turkish Chemical Society, Section B: Chemical Engineering, 7(1), 53–60. <https://doi.org/10.58692/jotcsb.1404612>.

\*Corresponding author. E-mail: [uner@metu.edu.tr](mailto:uner@metu.edu.tr).

### 1. INTRODUCTION

The importance of air separation arises from the necessity of supplying pure gases to chemical processes. Fresh air is almost 99% composed of nitrogen and oxygen, while the remaining is mainly argon along with some other noble gases and impurities. The details regarding the constituents of air can be seen in Table S.1 in the supplementary document. To the present day, the most successful method for air separation has been the cryogenic distillation of air, known as the air separation unit (ASU) in the chemical plants (Smith & Klosek, 2001). Cryogenic distillation proves effective in terms of providing excellent purity and achieving high production rates (Tesch et al., 2020). However, immense energy intensity associated with complexity of the liquefaction process and required

equipment make the cryogenic process unfavorable. In the cryogenic distillation, air is liquefied in a multi-step comprehensive process which includes compression, expansion, and heat exchangers leading to a limitation in thermodynamic second law efficiency to merely 25% (Krzystowczyk et al., 2021). On the other hand, CLAS is a self-contained air separation process working at atmospheric pressures and temperatures that can be achieved by focusing solar irradiation. According to a computational study performed by Li et. al., CLAS works on a specific energy consumption of 0.66 MJ/kg  $O_2$  while conventional cryogenic distillation consumes 0.78 MJ/kg  $O_2$  (Krzystowczyk et al., 2021). This implies a 15% decrease in energy consumption in the separation of air with further potential when it is coupled with solar energy.

Chemical looping air separation (CLAS) is an alternative to cryogenic separation, by utilizing solar thermal energy. In this process a reducible metal oxide is heated to a temperature where a lower oxidation state is more favorable, such that the metal oxide releases its lattice oxygen. In the second step, the metal oxide is exposed to air, and oxygen is captured by the oxide while pure nitrogen is released from the system and the loop is closed (Moghtaderi, 2010). The reactions for the proposed cycle are given below (K. Wang et al., 2013).

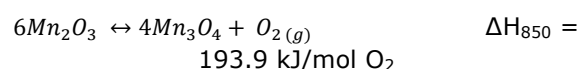


Although the pure and mixed metal oxides are evaluated in cyclic systems such as chemical looping oxygen uncoupling (CLOU) (Azimi et al., 2013; Shulman et al., 2011), and chemical looping combustion (CLC) (Abad et al., 2006; Adánez et al., 2018), CLAS seems to be the most sustainable solar energy storage method considering the product yield in the system (Bulfin et al., 2017). The simple design used in chemical looping air separation technology makes it more appealing for gas separation applications on a small scale (V. Shah et al., 2022). As a result of working at milder conditions and possible energy intensifications, its power consumption is lower than the conventionally used processes (Tao et al., 2022; K. Wang et al., 2016). Large scale applications of the CLAS process depend on selecting a convenient oxygen carrier and design of stable reactors that can withstand temperatures over 800 °C (Krzyszowczyk et al., 2021).

The most important aspects in the selection of the oxygen carrier are showing favorable reaction kinetics, transportation of oxygen with sufficient capacity, high mechanical and chemical resistance over repeated redox cycles, low cost, and environmental compliance. Manganese oxides in

this context are found sufficient to provide these effects in chemical looping air separation process by many researchers (K. Shah et al., 2012; Song et al., 2014; W. Wang et al., 2016; X. Wang et al., 2021). It is found that dual mixed and supported copper, cobalt, and manganese oxides can show promising results when performing redox cycles and to create a powerful alternative to cryogenic distillation (Moghtaderi, 2010). However, the performance of unsupported single metal oxides (especially Mn oxides) in the steam-air redox cycle is not investigated thoroughly in the literature.

At room temperature, the most stable form of manganese oxides is  $Mn_2O_3$  which reduces to  $Mn_3O_4$  at around 900 °C under air atmosphere. The reversible reaction of manganese oxides during the redox cycle is given as follows (Mattisson et al., 2009).



The reduction and oxidation of metal oxide can be triggered by inlet gas conditions in an isothermal process. Thus, energy and time saving in the process is improved by circumventing the time-consuming thermal transfer between the two steps of the cycle. The actual partial pressure of oxygen in the reaction chamber must be lower than its equilibrium value in order for the material to be stimulated to release oxygen to establish the equilibrium. Feed gas conditions for such stimulation include air at the oxidation step, and steam at the reduction step. Sweeping the oxygen in the reaction chamber with steam allows for a simple separation process of the product from the sweep gas. At a constant working temperature of 800-850 °C the material can be oxidized by air and reduced by steam. This method of pressure swing can facilitate the redox cycle by reducing the time needed to switch between reduction and oxidation, energy costs, and thermal stress on the material. The schematic of the proposed system is given in Figure 1.

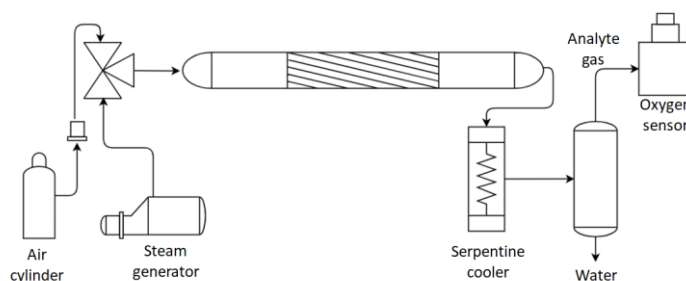


**Figure 1:** Chemical looping air separation experimental setup.

Coupling with solar energy will be accomplished by integrating the process into a parabolic mirror. These parabolic dishes are very successful in providing thermal energy with minimal losses since they directly concentrate the sun rays to the focal

point (Tescari et al., 2022). Reactor placement and focus adjustment are the crucial issues when coupling CLAS with solar energy (Khan et al., 2022; Patil et al., 2021). To utilize solar irradiation with

maximum efficiency, thermal losses should be minimized in the process.

## 2. EXPERIMENTAL SECTION

### 2.1. Materials

Manganese (II) oxide (MnO) is supplied from Aldrich Chemicals (99%, powder, -60 mesh). The material is used as is supplied commercially. Prior to the experiments, MnO is pre-oxidized under air flow.

### 2.2. Characterization

#### 2.2.1. Thermogravimetric Analysis (TGA)

Thermal gravimetric analysis experiments are conducted with Shimadzu DTG-60H TG/DTA. The redox behavior of the material under dry air (99.9%, Oksan) flow is investigated with a temperature profile of 1 °C/min up to 1000 °C.

#### 2.2.2. Cyclic TGA

To observe the reversibility of manganese oxides during the redox cycles, a cyclic analysis in TGA is performed. MnO is pre-oxidized to Mn<sub>2</sub>O<sub>3</sub> and the cycle starts. Temperature ramp is altered throughout the experiment. Additionally, hold times are added to promote complete reduction and oxidation at the respective stage.

#### 2.2.3. TGA Under Inert and Inert-Humidified Gas Conditions

To observe the effect of a non-oxidizing gas flow on the redox equilibrium, nitrogen gas (99.999%, Linde) is fed to the Mn<sub>2</sub>O<sub>3</sub> in the analysis chamber. Temperature profile is 5 °C/min up to 950 °C.

To reveal the effect of water vapor, nitrogen is passed through a wash bottle before entering the analysis chamber of the thermogravimetric analyzer. The temperature of the water in the wash bottle is adjusted to observe the effect of partial pressure of water in reduction of manganese oxides. Temperature profile is the same as dry nitrogen reduction. Wash bottle temperature is adjusted to 25 °C and 50 °C.

#### 2.2.4. Packed Bed Redox Cycle System

Manganese (II) oxide is filled into a quartz reactor and fixed by quartz wool. Length and overall diameter of the reactor are 600 mm and 12 mm respectively. Mass of MnO in the packing is 10 grams, corresponding to 0.14 moles. In the laboratory experiments, a homemade tubular oven is used to provide heat input to the system. Isothermal operation at 825 °C is conducted. Prior to

redox cycle, pre-oxidation of MnO to Mn<sub>2</sub>O<sub>3</sub> is carried out. During the oxidation cycle, material in the packing is oxidized under airflow at 80 mL/min feed rate from the dry air cylinder. The consecutive reduction cycle is accomplished by feeding steam into the reactor from a homemade steam generator.

### 2.3. Instruments

#### 2.3.1. Oxygen Sensor

A micro-fuel cell oxygen sensor module was procured from City Technologies company (model: CiTiceL AO2 Oxygen Sensor). Its circuit connections are assembled using an Arduino board and an additional ADS 1115 high-resolution analog-to-digital converter. For the measurement of oxygen concentration in a control volume, a polyamide block is carved, and a tee connection is built inside for the gas flow path and sensor junction. The block was carved such that the control volume was kept as small as possible to avoid a reduction in the sensitivity of the sensor along with an increase in response time.

#### 2.3.2. Steam Generator

The steam generator used in the system is built from the boiler of an out-of-use steam iron. The electronic connection of the boiler is separated from the iron so that the boiler works as a standalone steam generator. Steam output is directed into the system through a hose connection coupled with stainless steel junction at the end. The maximum power of the steam generator is 1400 W.

## 3. RESULTS AND DISCUSSION

### 3.1. Thermogravimetric Analyses

#### 3.1.1. Determination of The Working Capacity

The oxygen mobility on the material through the redox cycles can be screened via an observation over the mass of the oxygen carrier. Oxygen permeates through the lattice of manganese oxide until it reaches the saturation limit, so total mass of oxygen carrier is the main criterion that has influence on the overall capacity. The mass increase due to oxygen uptake for different phases of manganese oxides is given in Table 1. Calculation is based on stoichiometric reaction and mass balance, the details for the calculation can be found in supporting information document.

**Table 1:** Oxygen uptake of manganese oxides due to corresponding reactions.

Reaction	Oxygen Uptake (wt. %)
$3 \text{ MnO} + \frac{1}{2} \text{ O}_2 \rightarrow \text{ Mn}_3\text{O}_4$	7.52
$2 \text{ MnO} + \frac{1}{2} \text{ O}_2 \rightarrow \text{ Mn}_2\text{O}_3$	11.30
$\text{ MnO} + \frac{1}{2} \text{ O}_2 \rightarrow \text{ MnO}_2$	22.58

The calculation based on stoichiometric reactions will facilitate the comprehension of the materials phase conversion throughout the TGA experiments.

The result of thermogravimetric analysis to determine the working capacity is given in Figure 2.

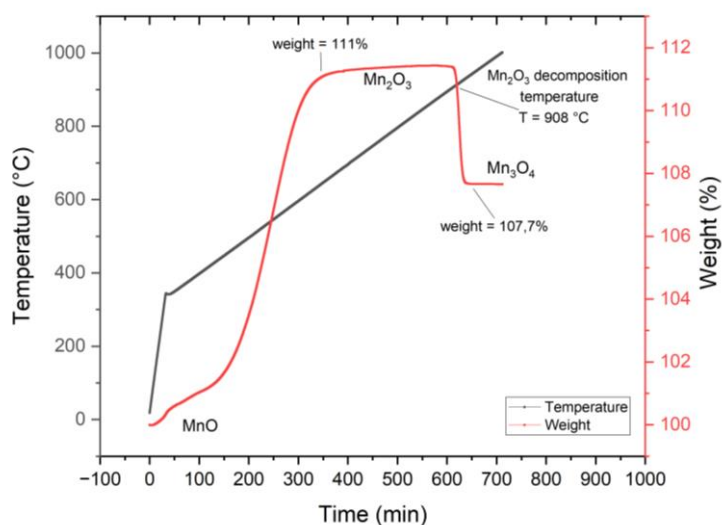


**Figure 2:** Thermogravimetric analysis for observation on working time capacity of manganese oxides.

Results obtained from TGA indicate that the weight change of the material complies with reaction stoichiometries as well as shift point temperatures dictated by thermodynamic limits. It is seen that the material is oxidized from rocksalt manganese (II) oxide to bixbyite (Mn<sub>2</sub>O<sub>3</sub>) up to a certain saturation level and the rate of oxidation then slows down. Oxidation occurs over a wide range of temperatures relying on the chemical kinetics stimulated by the increase in temperature while reduction to hausmannite (Mn<sub>3</sub>O<sub>4</sub>) is sharp and distinct driven by the thermodynamic limit that lies around 900 °C.

### 3.1.2. Reversible Interaction with Oxygen

When performing redox cycles with manganese oxides, it is possible to utilize temperature adjustments to induce the material to oxidize or reduce. Metal oxides usually prefer to be at a higher

oxidation state at lower temperatures, holding a greater amount of oxygen in their lattice. As the temperature goes up, the oxygen carrier tends to release oxygen driven by thermodynamic phase equilibrium. The crucial parameter is the reversibility of the material between reduced and oxidized phases over consecutive cycles. Manganese oxide is tested in a cyclic temperature profile to observe its reversible interaction with oxygen as well as if a change in the capacity occurs over successive cycles. Different heating rates, temperature intervals, and hold times are used to interactively reduce or oxidize the material when necessary. The results regarding the TGA for temperature induced redox cycle are given in Figure 3.

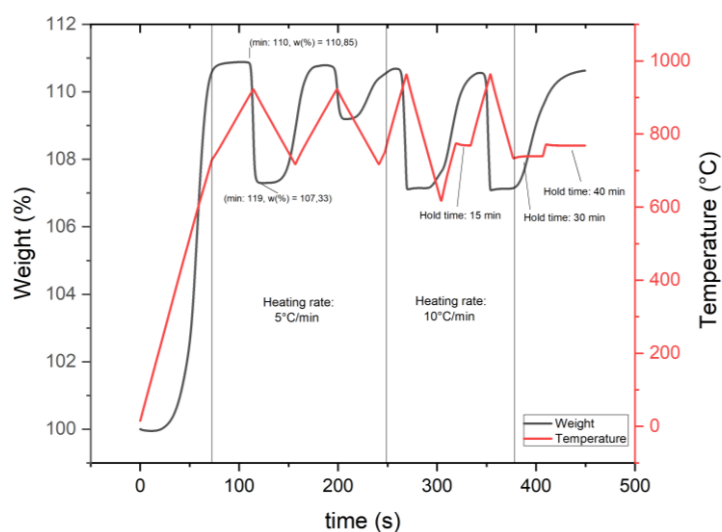


**Figure 3:** TGA cyclic temperature profile with manganese oxide.

### 3.1.3. Effect of Inert Atmosphere and Steam on Reduction

Previously oxidized manganese (II) oxide samples are reduced under the flow of dry and humidified N<sub>2</sub>. Oxidation is performed up to the Mn<sub>2</sub>O<sub>3</sub> phase. Humidification in the reduction stage is carried out

via wash bottles at 25 °C and 50 °C. The results are shown in Figure 4. It should be noted that prior to all reduction experiments, the material was oxidized to Mn<sub>2</sub>O<sub>3</sub> as indicated by weight increase in TGA and the profiles were identical.

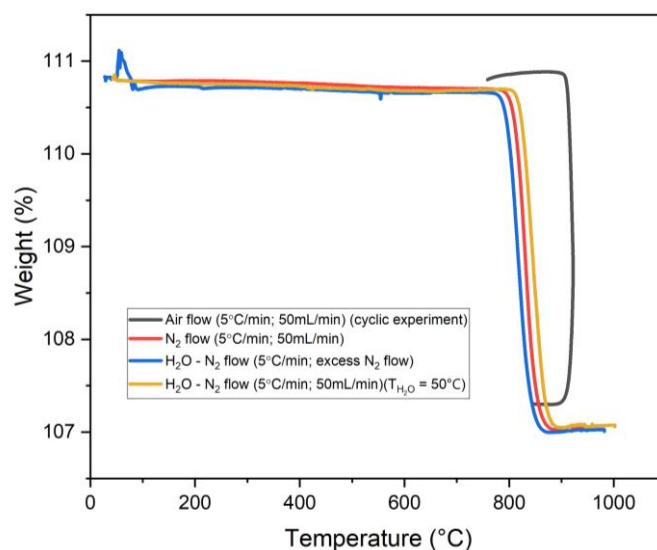


**Figure 4:** Mn<sub>2</sub>O<sub>3</sub> reduction profiles under different gas flow conditions.

It can be seen from the profiles that reduction under an inert atmosphere has resulted in a decrease in the reduction temperature to around 800 °C. Effect of inert and humidified gas conditions did not show great significance on the redox equilibria. It is demonstrated that water vapor acts as an inert gas at the reaction conditions and has a reducing effect on the material by sweeping the released oxygen from the reaction chamber.

### 3.2. Packed Bed Redox Cycle

The performance of manganese oxide packing in chemical looping air separation is tested by an oxidation step with air feed and a reduction step feeding steam into the reactor. The oxygen concentration in the output gas is monitored using a micro-fuel cell oxygen sensor. In the first step, starting material MnO is oxidized to Mn<sub>2</sub>O<sub>3</sub> with a temperature profile of 5 °C/min up to 850 °C under dry air feed at 80 mL/min. The results of the output gas concentration and the temperature profile in preliminary oxidation are given in Figure 5.

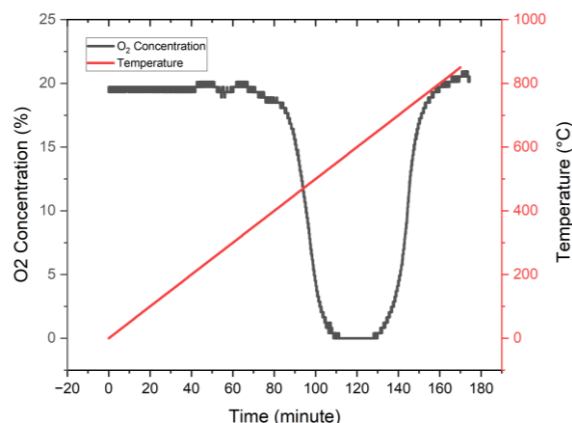


**Figure 5:** The oxygen concentration of the output gas and temperature profile during the oxidation of MnO to Mn<sub>2</sub>O<sub>3</sub>.

The result given in Figure 5 is an investigation on the output gas concentration when temperature programmed oxidation of MnO is carried out. From

the O<sub>2</sub> concentration results, it is seen that a gradual decrease in the beginning occurs due to the limitation in oxidation kinetics. With the increase in

the temperature, oxidation rate also increases, and all the incoming oxygen molecules are reacted with metal oxide packing, allowing for pure nitrogen production at the outlet. Total amount of oxygen that is absorbed is found to be 0.034 mol by the curve area which agrees well with the reaction stoichiometry. The details for the curve area calculation can be found in the supplementary document.

For the cyclic experiments, gas condition varied after the pre-oxidation of the material and a redox

cycle between  $Mn_2O_3$  and  $Mn_3O_4$  is performed. When the saturation of the material for oxygen is established as indicated by the equilibration of oxygen profile in the sensor, inlet gas is switched to steam to favor reduction of the metal oxide. Then, the gas condition is switched to air to re-oxidize the material, completing the cycle. The process is conducted isothermally at 825 °C. The result regarding the oxygen concentration profile during the redox cycle experiment is given in Figure 6.

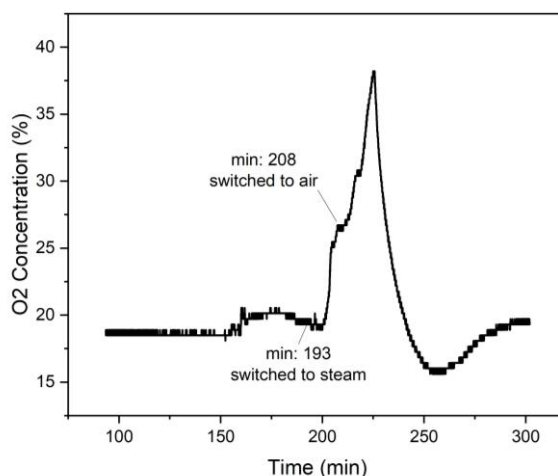


**Figure 6:** Oxygen concentration profile during redox cycle.

Steam flow started at a certain point for a 15-minute time interval. Due to the condensation units assembled after the reactor, steam condensed and did not sweep the oxygen gas further. Therefore, inlet gas condition is changed to air and a further sweep of the released oxygen is achieved. However, this caused simultaneous oxidation of the metal oxide bed that was oxygen deficit after a 15-min steam period.

The oxygen mobility on the material can be calculated by the peak area in the oxygen molar flow rate with respect to time plots. The procedure for the calculation of peak areas is given in supporting information. The results indicate that 0.0085 mol of oxygen is released during the reduction step. At the reoxidation step, 0.0053 mol

of oxygen is incorporated into the structure. Even if any simultaneous oxidation of the material is ignored, the oxygen release corresponds to 70 percent of the maximum capacity.

### 3.3. Parabolic Dish Power Measurements

The power output that can be obtained from a parabolic dish is tested with a 0.7 m diameter parabolic mirror. A water vessel with dimensions of 5 cm height and 2.5 cm diameter is insulated with a cordierite block and placed at the center of the focal point. A thermocouple is inserted in the water mass and the actual temperature is observed throughout the experiment. The resulting temperature profile is given in Figure 7.

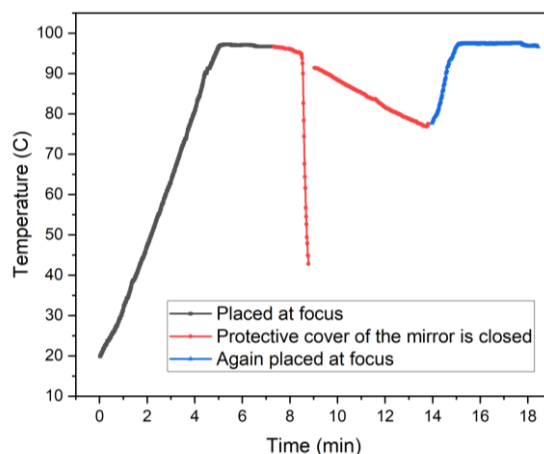


**Figure 7:** The temperature profile of water heated with parabolic mirror.

The power input is calculated as given in supplementary information with the help of the definite temperature ramp and known water mass. It is found that the parabolic mirror has provided the focus with 100 W of power. Considering that the solar energy available at the time of the experiment was 152 W, an irradiation efficiency of around 66% is achieved in the insulation system. The details of the calculation for the energy obtained with solar irradiation are given in supplementary information.

#### 4. CONCLUSION

Within the scope of the study, a unique reactor system is designed and constructed to perform redox cycles and test metal oxides for their performance in CLAS. The designed system led to the production of pure nitrogen at the outlet stream during the oxidation stage, and the production of oxygen at the reduction stage. The redox cycle is kept between  $Mn_2O_3$  and  $Mn_3O_4$  phases of manganese oxides. This is achieved by feeding air to oxidize, and steam to reduce the material at a constant temperature. The peak area calculations indicate that 0.034 mol oxygen is used in total throughout the oxidation of 10 g of manganese (II) oxide, which agrees well with the stoichiometric calculations. Considering that the redox cycle is performed between  $Mn_2O_3$  and  $Mn_3O_4$ , the capacity is 0.012 mol  $O_2$  per cycle, 10 g of oxide basis. The volume equivalent of this value results in a cycle capacity of 30 mL of  $O_2$  and 110 mL of  $N_2$  per gram of metal oxide. Moreover, the redox cycle experiments have revealed that at least 70 percent reduction is achieved under steam flow. However, since air is fed midway to reduction, simultaneous oxidation occurs while sweeping. Material re-oxidizes very slowly in the consecutive step since the condensation of water in the pipeline and wetted packing material cause an additional mass transfer, blocking the oxygen to penetrate through the lattice of the metal oxide. The use of superheated steam could be the solution to prevent this issue.

The possible practical applications of CLAS in the industry rely on studies that aim to discover

optimum operating conditions and materials that exhibit more favorable properties for the process. Since the CLAS allows the air separation process to be performed at a much smaller scale and under milder conditions, it is the most viable option for distributed plants that operate on renewable energy. Not only does it prove successful by opening a path where solar energy can be utilized to perform air separation, but it also offers advantages in terms of decreasing the specific energy consumption and reducing the fabrication costs for equipment.

#### 5. ACKNOWLEDGMENTS

State Oil Company of Azerbaijan Republic (SOCAR) is acknowledged for their partial financial support through the project code ODTU TTO GC-009-2022.

#### 6. REFERENCES

- Abad, A., Mattisson, T., Lyngfelt, A., & Rydén, M. (2006). Chemical-looping combustion in a 300 W continuously operating reactor system using a manganese-based oxygen carrier. *Fuel*, 85(9), 1174–1185. <https://doi.org/10.1016/j.fuel.2005.11.014>
- Adánez, J., Abad, A., Mendiara, T., Gayán, P., de Diego, L. F., & García-Labiano, F. (2018). Chemical looping combustion of solid fuels. In *Progress in Energy and Combustion Science* (Vol. 65, pp. 6–66). Elsevier Ltd. <https://doi.org/10.1016/j.peccs.2017.07.005>
- Azimi, G., Leion, H., Rydén, M., Mattisson, T., & Lyngfelt, A. (2013). Investigation of different Mn-Fe oxides as oxygen carrier for chemical-looping with oxygen uncoupling (CLOU). *Energy and Fuels*, 27(1), 367–377. <https://doi.org/10.1021/ef301120r>
- Bulfin, B., Vieten, J., Agrafiotis, C., Roeb, M., & Sattler, C. (2017). Applications and limitations of two step metal oxide thermochemical redox cycles; A review. In *Journal of Materials Chemistry A* (Vol. 5, Issue 36, pp. 18951–18966). Royal Society of Chemistry. <https://doi.org/10.1039/c7ta05025a>

- Khan, M. I., Asfand, F., & Al-Ghamdi, S. G. (2022). Progress in research and technological advancements of thermal energy storage systems for concentrated solar power. In *Journal of Energy Storage* (Vol. 55). Elsevier Ltd. <https://doi.org/10.1016/j.est.2022.105860>
- Krzystowczyk, E., Haribal, V., Dou, J., & Li, F. (2021). Chemical Looping Air Separation Using a Perovskite-Based Oxygen Sorbent: System Design and Process Analysis. *ACS Sustainable Chemistry and Engineering*, 9(36), 12185–12195. <https://doi.org/10.1021/acssuschemeng.1c03612>
- Mattisson, T., Lyngfelt, A., & Leion, H. (2009). Chemical-looping with oxygen uncoupling for combustion of solid fuels. *International Journal of Greenhouse Gas Control*, 3(1), 11–19. <https://doi.org/10.1016/j.ijggc.2008.06.002>
- Moghtaderi, B. (2010). Application of chemical looping concept for air separation at high temperatures. *Energy and Fuels*, 24(1), 190–198. <https://doi.org/10.1021/ef900553j>
- Patil, V. R., Kiener, F., Grylka, A., & Steinfeld, A. (2021). Experimental testing of a solar air cavity-receiver with reticulated porous ceramic absorbers for thermal processing at above 1000 °C. *Solar Energy*, 214, 72–85. <https://doi.org/10.1016/j.solener.2020.11.045>
- Shah, K., Moghtaderi, B., & Wall, T. (2012). Selection of suitable oxygen carriers for chemical looping air separation: A thermodynamic approach. *Energy and Fuels*, 26(4), 2038–2045. <https://doi.org/10.1021/ef300132c>
- Shah, V., Jangam, K., Joshi, A., Mohapatra, P., Falascino, E., & Fan, L. (2022). The Role of Chemical Looping in Industrial Gas Separation. In *Sustainable Separation Engineering* (pp. 199–237). Wiley. <https://doi.org/10.1002/9781119740117.ch5>
- Shulman, A., Cleverstam, E., Mattisson, T., & Lyngfelt, A. (2011). Chemical - Looping with oxygen uncoupling using Mn/Mg-based oxygen carriers - Oxygen release and reactivity with methane. *Fuel*, 90(3), 941–950. <https://doi.org/10.1016/j.fuel.2010.11.044>
- Smith, A. R., & Klosek, J. (2001). A review of air separation technologies and their integration with energy conversion processes. In *Fuel Processing Technology* (Vol. 70). www.elsevier.com/locate/proc
- Song, H., Shah, K., Doroodchi, E., Wall, T., & Moghtaderi, B. (2014). Reactivity of Al<sub>2</sub>O<sub>3</sub>- or SiO<sub>2</sub>-Supported Cu-, Mn-, and Co-based oxygen carriers for chemical looping air separation. *Energy and Fuels*, 28(2), 1284–1294. <https://doi.org/10.1021/ef402268t>
- Tao, Y., Tian, W., Kong, L., Sun, S., & Fan, C. (2022). Energy, exergy, economic, environmental (4E) and dynamic analysis based global optimization of chemical looping air separation for oxygen and power co-production. *Energy*, 261. <https://doi.org/10.1016/j.energy.2022.125365>
- Tescari, S., Neumann, N. C., Sundarraj, P., Moumin, G., Rincon Duarte, J. P., Linder, M., & Roeb, M. (2022). Storing solar energy in continuously moving redox particles – Experimental analysis of charging and discharging reactors. *Applied Energy*, 308. <https://doi.org/10.1016/j.apenergy.2021.118271>
- Tesch, S., Morosuk, T., & Tsatsaronis, G. (2020). Comparative Evaluation of Cryogenic Air Separation Units from the Exergetic and Economic Points of View. In *Low-temperature Technologies*. IntechOpen. <https://doi.org/10.5772/intechopen.85765>
- Wang, K., Yu, Q., Hou, L., Zuo, Z., Qin, Q., & Ren, H. (2016). Simulation and energy consumption analysis of chemical looping air separation system on Aspen Plus. *Journal of Thermal Analysis and Calorimetry*, 124(3), 1555–1560. <https://doi.org/10.1007/s10973-016-5237-9>
- Wang, K., Yu, Q., & Qin, Q. (2013). The thermodynamic method for selecting oxygen carriers used for chemical looping air separation. *Journal of Thermal Analysis and Calorimetry*, 112(2), 747–753. <https://doi.org/10.1007/s10973-012-2596-8>
- Wang, W., Zhang, B., Wang, G., & Li, Y. (2016). O<sub>2</sub> release of Mn-based oxygen carrier for chemical looping air separation (CLAS): An insight into kinetic studies. *Aerosol and Air Quality Research*, 16(2), 453–463. <https://doi.org/10.4209/aaqr.2014.07.0140>
- Wang, X., Shao, Y., & Jin, B. (2021). Thermodynamic evaluation and modelling of an auto-thermal hybrid system of chemical looping combustion and air separation for power generation coupling with CO<sub>2</sub> cycles. *Energy*, 236. <https://doi.org/10.1016/j.energy.2021.121431>